IRJSE International Research Journal of Science & Engineering
Int. Res. J. of Science & Engineering, Special Issue A12, February, 2023 SJIF Impact Factor 6.70
ISSN: 2322-0015 https://doi.org/10.5281/zenodo.7807209
RESEARCH ARTICLE OPEN ACCESS

The exploration and synthesis of perovskites $La_{0.2}Sr_{0.8}MnO_3$ electrode material for supercapacitor application.

Madhale KV[1], Faras MM[2], Mohite AA[2], Jamadar BN[3], Powar AA[3], Vhanakhande BB[3], Sapkal RT[4], Mane RD[4], Torane AP[2]*, Kulkarni SB[1]**

[1]Materials Research Laboratory, Department of Physics, The Institute of Science, Dr. Homi Bhabha State University, Madam Cama Road, Mumbai 400032, Maharashtra, India
[2]Department of Physics, Yashwantrao Chavan Institute of Science, Satara- 415001, Maharashtra, India
[3]Department of Humanities and Sciences, Walchand College of Engineering Sangli- 416416, Maharashtra, India
[4]Department of Physics, Tuljaram Chaturchand Collage of Arts, Science and Commerce Baramati- 413102, Maharashtra India
Corresponding author *Email: sbk_physics@yahoo.com | **appasahebtorane@yahoo.in

Manuscript Details
Available online on https://www.irjse.in
ISSN: 2322-0015

Cite this article as:
Madhale KV, Faras MM, Mohite AA, Jamadar BN, Powar AA, Vhanakhande BB, Sapkal RT, Mane RD, Torane AP, Kulkarni SB. The exploration and synthesis of perovskites $La_{0.2}Sr_{0.8}MnO_3$ electrode material for supercapacitor application, *Int. Res. Journal of Science & Engineering,* 2023, Special Issue A12: 55-64.
https://doi.org/10.5281/zenodo.7807209

Article published in Special issue of International Conference on "Recent Trends in Materials Science, Synthesis, Characterization and Applications (RTMS-2023)" organized by Department of Physics, Anekant Education Society's, Tuljaram Chaturchand College of Arts, Science and Commerce, Baramati, Dist Pune, Maharashtra, India (Autonomous) date, January 3-4, 2023.

Abstract

Herein, Agglomerated nanoflakes like perovskite lanthanum strontium manganite ($La_{0.2}Sr_{0.8}MnO_3$) material fabricated using an essential-route solution combustion method followed by a post-annealing procedure. Finally screen printed electrode used as the materials for high performance supercapacitors. The phase identification of Perovskite $La_{0.2}Sr_{0.8}MnO_3$ nanostructure was tested by X-ray diffractometer (XRD) and Fourier transform infrared (FT-IR) analysis confirms rhombohedral phase. Morphological studies were authenticated by Field emission scanning electron microscope (FE-SEM) showed that the well-developed agglomerated porous nanoflakes structured $La_{0.2}Sr_{0.8}MnO_3$ were prepared. Active surface area analysis was done by Brunauer–Emmett–Teller (BET) N_2 physisorption technique. The electrochemical properties of the screen-printed materials were tested using a three-electrode system. As a result, the perovskite $La_{0.2}Sr_{0.8}MnO_3$ electrode material showed a higher Csp of 710 F/g at a current density of 10 A/g within the potential range of -0.8 to 0.4 V in 1 M KOH electrolyte solution. In addition, the perovskite $La_{0.2}Sr_{0.8}MnO_3$ electrode material delivered excellent cycling stability, retaining 72.05 % of its initial Csp after 5000 successive cyclic voltammetry (CV) cycles. These results show that the unique solution combustion synthesized perovskite $La_{0.2}Sr_{0.8}MnO_3$ electrode material has remarkable application potential and can achieve better characteristics for high-performance supercapacitors in energy storage applications.

Keywords: Perovskite material, electrochemical measurements, nickel foam, Supercapacitor

Introduction

There is serious requirement for competent, clean, and sustainable energy sources, as well as new ideas regarding to energy conversion and storage, which deals with the express growth of the worldwide economy and the exhaustion of fossil fuels. In recent days, current energy storage devices represented by supercapacitors and rechargeable batteries have acquired positive regards for the sustainable advancement of resources and environment [1-4] Supercapacitors, also called electrochemical capacitors (ECs), are trending applications in various field like, hybrid electric vehicles, gigantic industrial instruments and renewable energy power plants.[5-7] Supercapacitors provide high power density, rapid charge/discharge, and long lifecycle as compared to traditional batteries. [8-11]. Meanwhile, ECs often have a poor energy density, which restricts the uses for them [12]. Many efforts are now being carried out to improve the energy density of supercapacitors. Although a wide operating voltage window (V) seems to be more important, a high specific capacitance (Csp) is still required for a maximum energy density (Ed) as of energy (E) obey the equation:

$$\mathbf{E} = \frac{1}{2}(\mathrm{Csp})\mathrm{V}^2 \qquad (1)$$

In practice, the electrode materials have a significant impact on the ECs electrochemical characteristics. As electrode materials for ECs, carbon materials, conductive polymers, and metal oxides [13-14]. have all been thoroughly investigated. These materials have a considerable impact on their electrochemistry and power density of ECs. The active component of electrode materials was given consideration, and it is often necessary for it to have a huge specific surface and strong electrical conductivity. Finding appropriate electrode materials is essential as it will boost the energy density by increasing potential windows along specific capacitance. The fact that transition metal oxides have a greater energy density than carbon materials and better stability than conducting polymers makes them desirable electrode materials in general.

Due to their unique electrical and magnetic transport properties along with other distinct features, the perovskites ABO_3-type ECs, where A and B stand for the 12 and 6 coordinated metals, have drawn a lot of attention. The B site is usually a transition metal element (Mn, Co, Ni, etc.), while the A site is typically a trivalent lanthanide ion (La^{3+}, Sm^{3+}, etc.) and/or a divalent alkaline earth ion (Sr^{2+}, Ba^{2+}, etc) [15-16]. Due to structural distortions, perovskites compounds have complicated structures that give rise to a wide range of linked pseudo-cubic structures like, monoclinic-orthorhombic-rhombohedral [17-19]. This uncertainty and magnetic characteristics perfectly count on the basis of synthesis parameters. Nowadays, Lanthanum strontium manganite ($La_{1-x}Sr_xMnO_3$) rare-earth perovskites material identified as the promising candidates because of their high redox activity and higher electrical conductivity than other transition metal oxides [20].

Based on earlier studies, we found the special structure of $La_{0.8}5Sr_{0.15}MnO_3$ has good mobility of ions and oxygens can increase conversion of Mn^{x+} to another valence state, having shown potential window of -0.8 to 0.5 V, but, poor electrical conductivity ulter its performance [21] Rare-earth manganites like $LnMnO_3$ contain hold trivalent metals. This makes the prepared structure more efficient systems for the investigation of multi-valent substitutions. In particular, the adjustment of La by Na or other alkali dopant metals influences structural, magnetic and other properties of resultant materials. $LaMnO_{3+\delta}$ is a admired perovskite structure, which can form with sub stoichiometric/super stoichiometric oxygen content, that is, $-0.25 \leq \delta \geq 0.25$ [22-23]. The lanthanum-based perovskite materials having improved electrical conductivity, wide potential window (> 1 V) and long cycling life. A regular approach to improve the electrical conductivity of La-based perovskites is by partially substitution of alkaline earth metal ($Ca^{2þ}$, $Sr^{2þ}$ etc.), through which more oxygen vacancies are introduced. Hence, it modified capacitive performance of ECs [24-26]. The potential use of mixed-valent perovskite with trivalent lanthanide ion in the A site is extensively studied as supercapacitor electrode [26-28]. Doping in these perovskite materials, where the

divalent Sr ion introduced in La-based perovskite lattice magnify the ECs performance.

In this work, we synthesized $La_{0.2}Sr_{0.8}MnO_3$ perovskite electrode material containing a mesoporous structure by the unique solution combustion method. In this synthesis technique citric acid is used as fuel. Finally collected sample was screen printed on nickel foam substrate. Solution combustion route is versatile method for in-situ doping of various metals. Also, help to form well-developed porosity of active electrode materials by gas evolution during synthesis. This method provides nanocrystalline $La_{0.2}Sr_{0.8}MnO_3$ structure. The effect of synthesis strategy is throughout studied. This work may provide a new way to synthesize other ABO_3-type perovskite electrode material for supercapacitor application.

Methodology

1. Chemicals

Lanthanum nitrate [$La(NO_3)_3.6H_2O$], strontium nitrate [$Sr(NO_3)_2$], manganese nitrate [$Mn(NO_3)_2.4H_2O$], citric acid [$C_6H_8O_7$], N-methyl-2-pyrrolidone (NMP), Carbon black, Poly-vinylidene fluoride (PVDF) and potassium hydroxide (KOH) were purchased from Thomas baker (India). Ni foam was purchased from Vritra Technologies, India. All chemicals were analytical grade and used without any purification. Double-distilled water (DDW) was used as a solvent throughout the experiments.

2. Synthesis

We have synthesized Perovskites $La_{0.2}Sr_{0.8}MnO_3$ by solution combustion synthesis method. To prepare $La_{0.2}Sr_{0.8}MnO_3$, stoichiometric amounts of 0.86 gm of lanthanum nitrate $La(NO_3)_3.6H_2O$, 1.69 gm of $Sr(NO_3)_2$, 2.51 gm of $Mn(NO_3)_2.4H_2O$, and 1.92 gm of $C_6H_8O_7$ were used as precursor materials. At first, the $La(NO_3)_3.6H_2O$, $Sr(NO_3)_2$ and $Mn(NO_3)_2.4H_2O$ were dissolved in 100 ml DDW separately to form 0.1 M solution. The equimolar solution of $C_6H_8O_7$ was also prepared in the DDW and used as fuel for reaction. These solutions were mixed in each other and ultrasonic treatment was given to this uniform solution for 15 min. afterwards mixture was kept onto a magnetic stirrer for 40 min to get a uniform solution. Finally, the mixture was kept on a heating coil for proceed the burning process. Resultantly, we get the output product in the form of ash of $La_{0.2}Sr_{0.8}MnO_3$ with N_2 and CO_2 along with vapours of H_2O. The prepared sample was ground in agate mortar and followed sintering treatment at 700 ^{0}c for 4 hrs.

3. Characterization Techniques

The phase identification of the prepared sample was confirmed via X-ray Diffraction (XRD) technique at a scan rate of 2^o s^{-1}. For surface analysis and elemental analysis, Field-Emission Scanning Electron Microscopy along with Energy Dispersive spectroscopy (FESEM, EDAX) were run. To examine the surface area and porosity, Brunauer–Emmett–Teller (BET) was tested. Raman spectroscopy was used for getting bonding information between metals.

4. Electrochemical testing and electrode fabrication

The electrochemistry of Perovskites $La_{0.2}Sr_{0.8}MnO_3$ electrode was done by using the cyclic voltammogram (CV), galvanostatic charge-discharge (GCD), electrochemical impedance spectroscopy (EIS) measurements, which were carried out (Met Rohm auto lab PGSTAT302N) in a 1 M KOH electrolyte. All measurements were carried out in three electrodes system at room temperature. The prepared $La_{0.2}Sr_{0.8}MnO_3$ electrode was taken as a working electrode (WE), graphite was used as the counter electrode (CE), and saturated calomel electrode (SCE) employed as a reference electrode (RE). The electrode was prepared by taking active material $La_{0.2}Sr_{0.8}MnO_3$, carbon black (CB), and poly-vinylidene fluoride (PVDF) at an 8:1:1 ratio, and N-Methyl-2-Pyrrolidone (NMP) liquid was used to make the slurry this slurry was screen printed on Ni foam substrate, after drying overnight at 60 °C the electrode was tested.

Result and Discussion

3.1 XRD

The XRD study for the perovskite $La_{0.2}Sr_{0.8}MnO_3$ sample was carried out to identify composition and phase structure. Crystallinity and BET area are the factors that

influence the electrochemistry of electrode material [29]. From Fig. 1(a) it can be shown that there are mainly eight diffracted peaks at 2Θ angles of 32.54°, 40.13°, 43.13°, 46.92°, 58.31°, 68.62°, 78.03° and 82.5° respectively, corresponding crystal planes are (110), (202), (006), (024), (214), (208), (128) and (026). All peaks are well indexed to the rhombohedral $La_{0.2}Sr_{0.8}MnO_3$ phase as compared with the standard JCPDS card no. 00-050-0308 with the R-3C space group. There is no secondary phase that appears in the XRD plot of the perovskite, which indicates high purity of the $LaSrMnO_3$ material. Scherrer analysis of the peak at 32.54° determined an average crystalline domain of 11.24 nm for $La_{0.2}Sr_{0.8}MnO_3$ sample. In addition, the lattice parameters of the perovskite were found to be a = b = 5.49 Å, c = 13.35 Å, α = β = 90°, γ = 120° obtained from XRD data.

3.2 FTIR

The presence of functional groups in the $La_{0.2}Sr_{0.8}MnO_3$ sample was confirmed by FTIR spectroscopy. The perovskite powder was sintered at 700 °C and FTIR was taken as shown in Fig 1 (b). The absorption peaks of $La_{0.2}Sr_{0.8}MnO_3$ were seen within the wave number region of 4000 to 400 cm^{-1}. The plot located a sharp adsorption peak around 601.75 cm^{-1} as a result of (Mn-O) metal-oxygen vibrations frequency and the formation of $LaSrMnO_3$ perovskite structure. Also, the characteristic absorptions of the carbonates are displayed at 1450.05 cm^{-1} and 2920.5 cm^{-1} respectively, implying traces of carboxyl groups (C=O) [30]. The prominent absorption in the range of 3282–3644 cm^{-1}, corresponding to the H – O–H stretching can be ascribed to the chemisorbed water content [31]. As a result, the FTIR analysis of $LaSrMnO_3$ powder agrees with the XRD data.

3.3 FE-SEM with EDAX

Fig 2 (a-d) shows the FE-SEM images of $La_{0.2}Sr_{0.8}MnO_3$ perovskite at different magnifications (25 kX to 100 kX) and 15 kV operating voltage to comprehend the $La_{0.2}Sr_{0.8}MnO_3$ sample's morphologies better. From the figure, it can be seen that $La_{0.2}Sr_{0.8}MnO_3$ powder was an almost agglomerated nanoflakes-like morphology. This nanoflakes clusters images reveal a mesoporous, non-homogeneous random grain size distribution. This leads to easy contact between the electrolyte and the active site, facilitating penetration of the electrolyte. Which results in low impedance and modified ion/electron transportation.

For knowing the elemental composition of the $La_{0.2}Sr_{0.8}MnO_3$ sample is scanned by the EDAX analysis. Moreover, the EDX spectrum of perovskite $LaSrMnO_3$ material confirmed the existence of La, Sr, Mn and O elements. The table of numerical results in the inset gives all details numbers in weight and atomic percentage of the $LaSrMnO_3$ sample. It explained that perovskite $LaSrMnO_3$ sample does not have any impurity and it is well stoichiometric by nature.

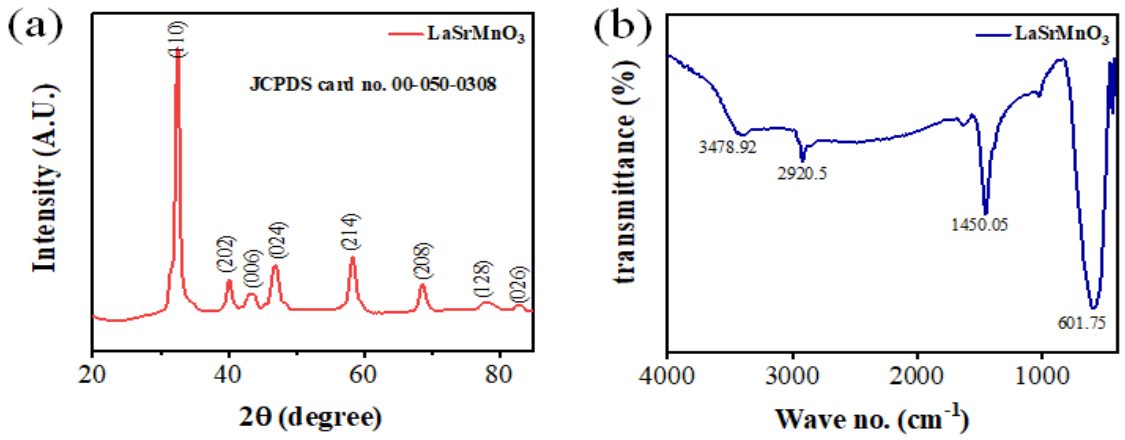

Fig. 1: (a) XRD plot of the $LaSrMnO_3$ sample and (b) FTIR spectra of the $LaSrMnO_3$ material.

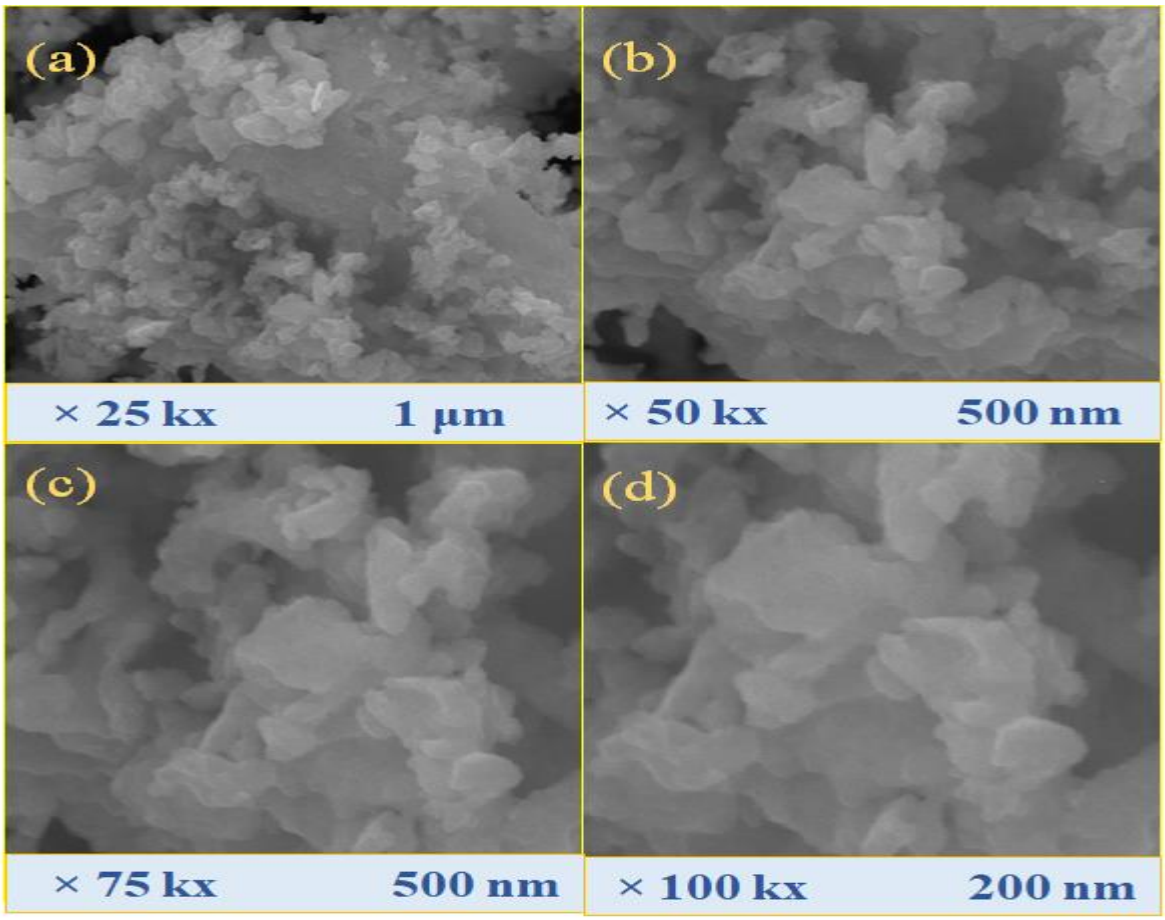

Fig. 2: FESEM micrographs of the $LaSrMnO_3$ Nano powder.

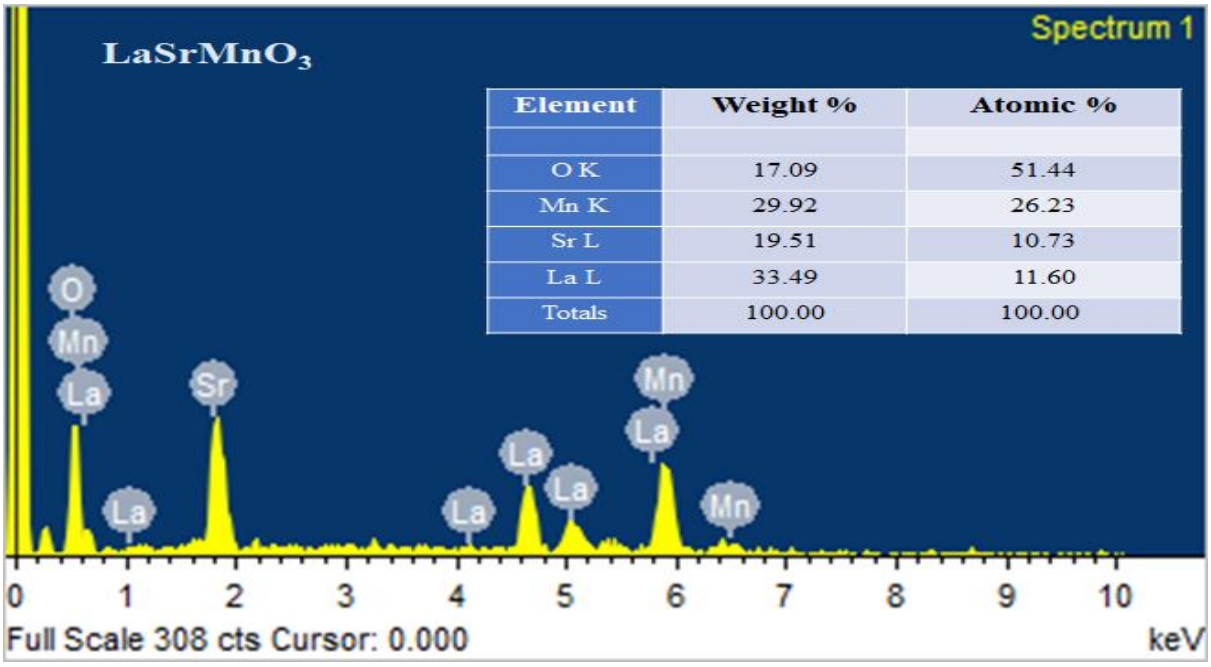

Fig. 3: EDAX analysis of the $LaSrMnO_3$ sample.

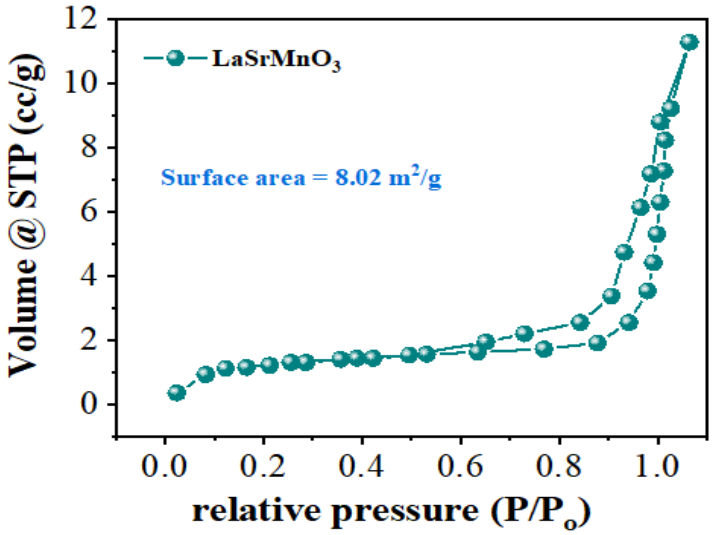

Fig. 4: BET analysis of the $LaSrMnO_3$ material.

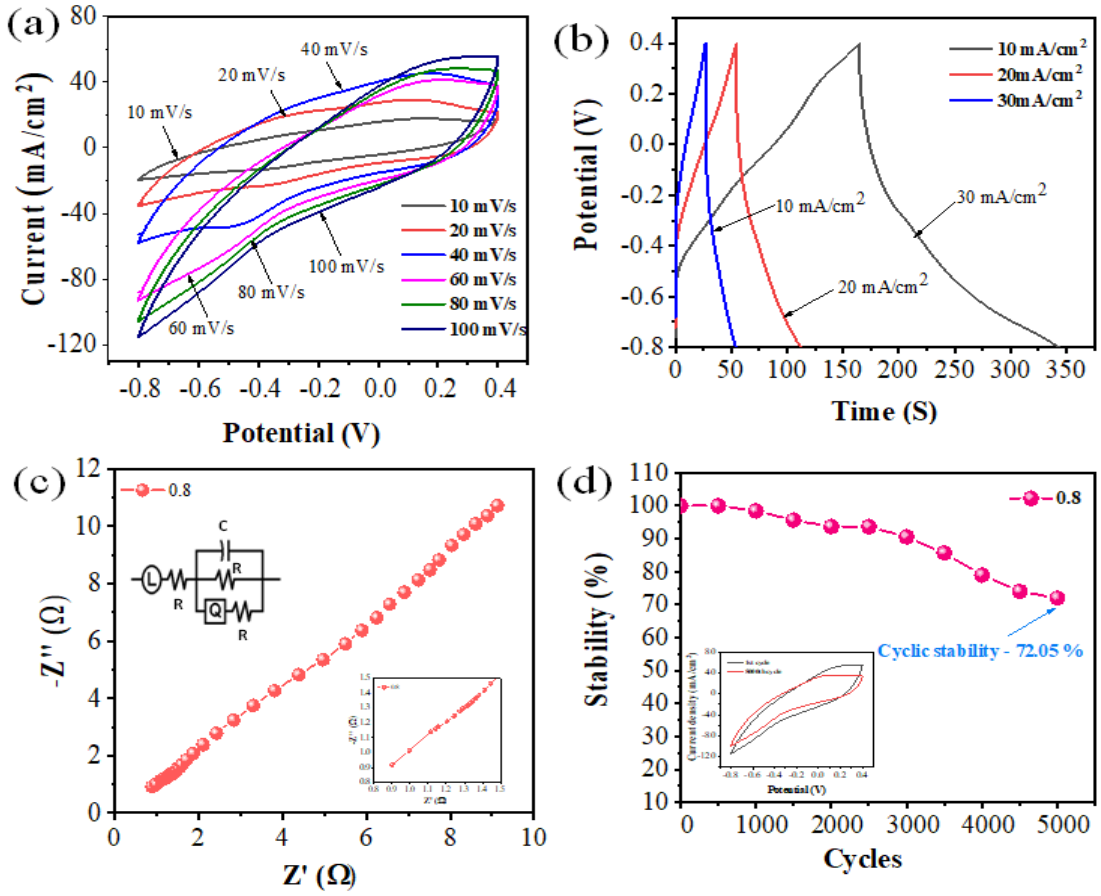

Fig. 5: Electrochemical analysis of perovskite $LaSrMnO_3$ electrode (a) CV at different scan rates (10-100 mV/s), (b) GCD at different current densities (10, 20 and 30 mA/cm²), (c) Nyquist plot and (d) Cyclic stability curve in 1 M KOH aqueous electrolyte.

Table 1: Table of electrochemical results of $LaSrMnO_3$ electrode.

Sample code	Specific capacitance (F/g)	Energy density (Wh/kg)	Power density (W/kg)
$La_{0.2}Sr_{0.8}MnO_3$	710	142	2857

Table 2: Table of the rate capability measurements of the $LaSrMnO_3$ electrode.

Discharge current (Id) (mA/cm^2)	Specific capacitance (F/g)	Rate capability (%)
10	710	-
20	532.6	74.9
30	441.3	62.1

Table 3: Comparison of $LaSrMnO_3$ electrode with other reported literature.

Sr. No.	Electrode	Electrolyte	Potential window	Surface area	Specific capacitance	Cyclic stability	Ref.
1	LZCS	1 M KOH	0 to 0.6 V	-	83.3 F/g at 10 mV/s	-	https://doi.org/10.1016/j.matchemphys.2019.05.083
2	$LaMnO_{2.97}$	1 M KOH	-1.2 to 0.0 V	10.6 m^2/g	609.8 F/g at 2 mV/s	-	10.1038/nmat4000
3	LaMnO3	6 M KOH	0 to 1 V	42 m2 /g	40 F/g at a discharge of up to 1V.	-	10.15330/pcss.21.2.219-226
4	$La_{0.7}Sr_{0.3}MnO_3$	1 M KOH	-0.6 to 0.6	46.7 m^2/g	73.2 F/g at 5 mV/s	-	https://doi.org/10.1016/j.ceramint.2021.02.160
5	$La_{0.85}Sr_{0.15}MnO_3$	1 M KOH	-0.96 to 0.65 V	-	198 F/g at 0.5 A/g	-	https://doi.org/10.1016/j.jallcom.2016.03.048
6	**$La_{0.2}Sr_{0.8}MnO_3$**	**1 M KOH**	**-0.8 to 0.4**	**8.02 m^2/g**	**710 F/g at 10 mA/ cm^2**	**72.05 % after 5,000 cycles**	**This work**

Table 4: Values of $Total\ R, L, Q$ and C obtained from the Z fitting method based on the matched equivalent circuit.

Sample Code	L (H)	R (Ω)	C (mF)	Q
$LaSrMnO_3$	5.2	16.6	0.24	0.006

3.4 BET

BET analysis were carried out to obtain the surface area, pore diameter, and pore volume of the perovskite $La_{0.2}Sr_{0.8}MnO_3$ sample [32]. Fig. 4 demonstrate N_2 physisorption isotherm analysis of perovskite samples measured within the relative pressure range of 0 to 1.0 at 77K. According to modern nomenclature system, $LaSrMnO_3$ sample show type III isotherm which explained less adsorbate-adsorbate interactions. The pore volume was calculated using standard BJH method. The specific surface area of $La_{0.2}Sr_{0.8}MnO_3$ sample was found to be 8.02 m^2/g and pore volume was calculated to be 0.41 cm^3/g. Which is typical feature of micropores. This micropores can be formed due to decomposition of lanthanum-strontium-manganese precursors during ash formation process. The poor surface area may result due to high annealing temperature, (700 °C) which reduce extensive growth of

the perovskite $La_{0.2}Sr_{0.8}MnO_3$ and the alter of the pore network [33].

3.5 Electrochemical measurements

The surface morphology and structure of material significant effect on the electrochemistry of sample. A maximum current and a rectangular shape of CV, symmetry in anodic and cathodic directions, are the fingerprints of ideal behaviour of capacitive electrode. Fig. 5 (a) shows CV of perovskite $La_{0.2}Sr_{0.8}MnO_3$ electrode supported by NF was recorded in three-electrode system. The measurement was carried out in 1 M KOH electrolyte at different scan rates of 10-100 mV/s in a potential window of −0.8 to 0.4 V vs SCE. As shown in Fig. 5 (a), the enclosed area of the perovskite $La_{0.2}Sr_{0.8}MnO_3$ electrode is obviously larger than that of $LaMnO_3$ and $SrMnO_3$ [34]. This increased area of $La_{0.2}Sr_{0.8}MnO_3$ is mainly come up with synergistic effects between $LaMnO_3$ and $SrMnO_3$ [29]. The rectangular shape of the CV curve is almost maintained even at higher sweep rate exhibit mirror-image characteristics of material, which explain the rate capability of the perovskite electrode. Possible reaction mechanism that may occurs can deduced as follows;

$$0.2La(NO_3)_3 + 0.8Sr(NO_3)_2 + Mn(NO_3)_2.4H_2O + C_6H_8O_7 \rightarrow La_{0.2}Sr_{0.8}MnO_3 + 8H_2O + 2.2N_2 + 6CO_2 + 1.2[O] \quad (2)$$

To explore further $La_{0.2}Sr_{0.8}MnO_3$ perovskite material as an efficient supercapacitor electrode, GCD was carried out at various current densities. Figure 5 (b) shows the comparative GCD curves of $La_{0.2}Sr_{0.8}MnO_3$ electrode obtained at different current densities of 10-30 mA/cm². Triangular symmetry and linear charge-discharge behaviour evident the pseudocapacitive nature of the perovskite sample. The slight deviation of the curves from its shape (Fig. 5 (b)) is considered to be related with the equivalent series resistance (Rs) between electrode-electrolyte interface [35]. The charge storage capability of the $La_{0.2}Sr_{0.8}MnO_3$ electrode was calculated from the GCD curve by using following formulae (3), (4) and (5) and the results are included in table 1.

$$\text{Specific Capacitance(Csp)}\left(\frac{F}{g}\right) = \frac{I_d(A) \times T_d(s)}{m\,(g) \times dV(V)} \quad (3)$$

$$\text{Energy Density (E.D.)} = \frac{1}{2} \times Csp \times (dV)^2 \quad (4)$$

$$\text{Power Density (P.D.)} = \frac{E.D.}{Td} \quad (5)$$

To study rate capability GCD was carried out at 10, 20 and 30 mA/cm² (fig.5 (b)) and results are tabulated in Table 2. From the table, Csp of perovskite $La_{0.2}Sr_{0.8}MnO_3$ electrode is retained by an amount of 62.1 % at 30 mA/cm² in comparison with the Csp at 10 mA/cm².

Electrochemical impedance spectroscopy (EIS) was run in the frequency range of 0.01 Hz to 100 kHz for same material and results are listed in table 4. EIS Fig 5 (c) shows charge transfer kinetics of perovskite $La_{0.2}Sr_{0.8}MnO_3$ sample. Cyclic stability is the key point to test electrode material in electrochemical field. To examine durability of perovskite material, cyclic stability of $La_{0.2}Sr_{0.8}MnO_3$ sample was recorded over 5,000 CV cycles at 100 mV/s scan rate. As shown in Fig 5 (d) initially Csp of first 1,000 cycles was remains same; after that, Csp was relatively decreasing. It may due to diffusion at electro-active interface. From this test, $La_{0.2}Sr_{0.8}MnO_3$ electrode shows 72.05 % retention of capacitance after successive 5,000 CV cycles. From all the results and measurements, it can be concluded that perovskite $La_{0.2}Sr_{0.8}MnO_3$ sample can be one of the promising and excellent electro-active material for future supercapacitors application

Conclusions

In conclusion, we have successfully synthesized perovskite $La_{0.2}Sr_{0.8}MnO_3$ nanoflakes through a facile solution combustion route followed by annealing treatment. The optimal concentration of precursors significantly affected the electrical conductivity of

$La_{0.2}Sr_{0.8}MnO_3$ samples. Owing to the nanostructures and higher electrical conductivity, as prepared perovskite $La_{0.2}Sr_{0.8}MnO_3$ nanoflakes delivered a high Csp of 710 F/g at 10 mA/cm^2 in 1 M KOH. In addition, $La_{0.2}Sr_{0.8}MnO_3$ electrode shows 72.05 % cyclic durability after 5,000 CV cycles at a 100 mV/s scan rate. Along with, perovskite delivers 142 Wh/kg energy density and 2857 W/kg power density, respectively. Therefore, we can say that prepared perovskite $La_{0.2}Sr_{0.8}MnO_3$ nanoflakes electrodes are suitable for supercapacitor fabrication.

Declaration of Competing Interest

The authors declare that they have no known competing financial interests or personal relationships that could have appeared to influence the work reported in this paper.

Acknowledgments

Authors Ms. M. M. Faras and Mr. A. A. Mohite would like to acknowledge to MJPRF-2021 Government of Maharashtra, India. for providing financial assistance.

References

1. M. R. Lukatskaya, B. Dunn, and Y. Gogotsi, "Multidimensional materials and device architectures for future hybrid energy storage," Nat. Commun., vol. 7, 2016, doi: 10.1038/ncomms12647.
2. M. Zhi, C. Xiang, J. Li, M. Li, and N. Wu, "Nanostructured carbon-metal oxide composite electrodes for supercapacitors: A review," Nanoscale, vol. 5, no. 1, pp. 72–88, 2013, doi: 10.1039/c2nr32040a.
3. P. P. Ma et al., "Flexible supercapacitor electrodes based on carbon cloth-supported lamno3/mno nano-arrays by one-step electrodeposition," Nanomaterials, vol. 9, no. 12, 2019, doi: 10.3390/nano9121676.
4. Y. Luo et al., "Seed-assisted synthesis of highly ordered TiO2α- Fe 2O3 core/shell arrays on carbon textiles for lithium-ion battery applications," Energy Environ. Sci., vol. 5, no. 4, pp. 6559–6566, 2012, doi: 10.1039/c2ee03396h.
5. J. Zhang and X. S. Zhao, "On the configuration of supercapacitors for maximizing electrochemical performance," ChemSusChem, vol. 5, no. 5, pp. 818–841, 2012, doi: 10.1002/cssc.201100571.
6. G. Wang, L. Zhang, and J. Zhang, "A review of electrode materials for electrochemical supercapacitors," Chem. Soc. Rev., vol. 41, no. 2, pp. 797–828, 2012, doi: 10.1039/c1cs15060j.
7. T. Brousse et al., "Materials for electrochemical capacitors," Springer Handbooks, pp. 495–561, 2017, doi: 10.1007/978-3-662-46657-5_16.
8. M. Jayalakshmi and K. Balasubramanian, "Simple capacitors to supercapacitors - An overview," Int. J. Electrochem. Sci., vol. 3, no. 11, pp. 1196–1217, 2008.
9. A. Lahyani, P. Venet, A. Guermazi, and A. Troudi, "Battery/Supercapacitors Combination in Uninterruptible Power Supply (UPS)," IEEE Trans. Power Electron., vol. 28, no. 4, pp. 1509–1522, 2013, doi: 10.1109/TPEL.2012.2210736.
10. A. Kuperman and I. Aharon, "Battery-ultracapacitor hybrids for pulsed current loads: A review," Renew. Sustain. Energy Rev., vol. 15, no. 2, pp. 981–992, 2011, doi: 10.1016/j.rser.2010.11.010.
11. Y. Zhang et al., "Progress of electrochemical capacitor electrode materials: A review," Int. J. Hydrogen Energy, vol. 34, no. 11, pp. 4889–4899, 2009, doi: 10.1016/j.ijhydene.2009.04.005.
12. J. Xie, P. Yang, Y. Wang, T. Qi, Y. Lei, and C. M. Li, "Puzzles and confusions in supercapacitor and battery: Theory and solutions," J. Power Sources, vol. 401, no. December 2017, pp. 213–223, 2018, doi: 10.1016/j.jpowsour.2018.08.090.
13. S. Bose, T. Kuila, A. K. Mishra, R. Rajasekar, N. H. Kim, and J. H. Lee, "Carbon-based nanostructured materials and their composites as supercapacitor electrodes," J. Mater. Chem., vol. 22, no. 3, pp. 767–784, 2012, doi: 10.1039/c1jm14468e.
14. G. A. Snook, P. Kao, and A. S. Best, "Conducting-polymer-based supercapacitor devices and electrodes," J. Power Sources, vol. 196, no. 1, pp. 1–12, 2011, doi: 10.1016/j.jpowsour.2010.06.084.
15. R. M. Kusters, J. Singleton, D. A. Keen, R. McGreevy, and W. Hayes, "Magnetoresistance measurements on the magnetic semiconductor Nd0.5Pb0.5MnO3," Phys. B Phys. Condens. Matter, vol. 155, no. 1–3, pp. 362–365, 1989, doi: 10.1016/0921-4526(89)90530-9.
16. X. Lang, H. Mo, X. Hu, and H. Tian, "Supercapacitor performance of perovskite La1-: XSrxMnO3," Dalt. Trans., vol. 46, no. 40, pp. 13720–13730, 2017, doi: 10.1039/c7dt03134c.
17. M. V. Kuznetsov, I. P. Parkin, D. J. Caruana, and Y. G. Morozov, "Combustion synthesis of alkaline-earth substituted lanthanum manganites; LaMnO3, La0.6Ca0.4MnO3and La0.6Sr0.4MnO3," J. Mater. Chem., vol. 14, no. 9, pp. 1377–1382, 2004, doi: 10.1039/b313553p.

18. J. Mitchell, D. Argyriou, C. Potter, D. Hinks, J. Jorgensen, and S. Bader, "Structural phase diagram of: Relationship to magnetic and transport properties," Phys. Rev. B - Condens. Matter Mater. Phys., vol. 54, no. 9, pp. 6172–6183, 1996, doi: 10.1103/PhysRevB.54.6172.
19. J. S. White, "Single Crystals," Rocks Miner., vol. 81, no. 6, pp. 471–472, 2006, doi: 10.3200/rmin.81.6.471-472.
20. S. Takenoiri, N. Kadokawa, and K. Koseki, "Development of metallic substrate supported planar solid oxide fuel cells fabricated by atmospheric plasma spraying," J. Therm. Spray Technol., vol. 9, no. 3, pp. 360–363, 2000, doi: 10.1361/105996300770349809.
21. X. Lang et al., "Ag nanoparticles decorated perovskite La 0.85 Sr 0.15 MnO 3 as electrode materials for supercapacitors," Mater. Lett., vol. 243, pp. 34–37, 2019, doi: 10.1016/j.matlet.2019.02.002.
22. R. Cortés-Gil et al., "Evolution of magnetic behaviour in oxygen deficient LaMnO 3-δ," J. Phys. Chem. Solids, vol. 67, no. 1–3, pp. 579–582, 2006, doi: 10.1016/j.jpcs.2005.10.122.
23. R. Laiho et al., "Low-field magnetic properties of LaMnO3+δ with 0.065 ≤ δ ≤ 0.154," J. Phys. Chem. Solids, vol. 64, no. 12, pp. 2313–2319, 2003, doi: 10.1016/S0022-3697(03)00266-X.
24. A. Roy et al., "Supercapacitor performance of perovskite La1-: XSrxMnO3," Electrochim. Acta, vol. 343, no. 9, pp. 13720–13730, 2019, doi: 10.1016/j.mattod.2018.11.002.
25. Y. Cao, B. Lin, Y. Sun, H. Yang, and X. Zhang, "Symmetric/Asymmetric Supercapacitor Based on the Perovskite-type Lanthanum Cobaltate Nanofibers with Sr-substitution," Electrochim. Acta, vol. 178, pp. 398–406, 2015, doi: 10.1016/j.electacta.2015.08.033.
26. H. Mo et al., "Influence of calcium doping on performance of LaMnO3 supercapacitors," Ceram. Int., vol. 44, no. 8, pp. 9733–9741, 2018, doi: 10.1016/j.ceramint.2018.02.205.
27. Y. Guo, T. Shao, H. You, S. Li, C. Li, and L. Zhang, "Polyvinylpyrrolidone-assisted solvothermal synthesis of porous LaCoO3 nanospheres as supercapacitor electrode," Int. J. Electrochem. Sci., vol. 12, no. 8, pp. 7121–7127, 2017, doi: 10.20964/2017.08.47.
28. J. T. Mefford, W. G. Hardin, S. Dai, K. P. Johnston, and K. J. Stevenson, "Anion charge storage through oxygen intercalation in LaMnO 3 perovskite pseudocapacitor electrodes," Nat. Mater., vol. 13, no. 7, pp. 726–732, 2014, doi: 10.1038/nmat4000.
29. P. Goel et al., "Perovskite materials as superior and powerful platforms for energy conversion and storage applications," Nano Energy, vol. 80, p. 105552, 2021, doi: 10.1016/j.nanoen.2020.105552.
30. A. O. Turky, M. M. Rashad, A. M. Hassan, E. M. Elnaggar, and M. Bechelany, "Optical, electrical and magnetic properties of lanthanum strontium manganite La1-xSrxMnO3 synthesized through the citrate combustion method," Phys. Chem. Chem. Phys., vol. 19, no. 9, pp. 6878–6886, 2017, doi: 10.1039/c6cp07333f.
31. Z. X. Wei, L. Wei, L. Gong, Y. Wang, and C. W. Hu, "Combustion synthesis and effect of LaMnO3 and La0.8Sr0.2MnO3 on RDX thermal decomposition," J. Hazard. Mater., vol. 177, no. 1–3, pp. 554–559, 2010, doi: 10.1016/j.jhazmat.2009.12.068.
32. B. M. Kim, H. Y. Kim, S. W. Hong, W. H. Choi, Y. W. Ju, and J. Shin, "Structurally distorted perovskite La0.8Sr0.2Mn0.5Co0.5O3-δ by graphene nanoplatelet and their composite for supercapacitors with enhanced stability," Sci. Rep., vol. 12, no. 1, pp. 1–8, 2022, doi: 10.1038/s41598-022-14324-5.
33. X. Xiao, B. Peng, L. Cai, X. Zhang, S. Liu, and Y. Wang, "The high efficient catalytic properties for thermal decomposition of ammonium perchlorate using mesoporous ZnCo2O4 rods synthesized by oxalate co-precipitation method," Sci. Rep., vol. 8, no. 1, pp. 1–13, 2018, doi: 10.1038/s41598-018-26022-2.
34. P. M. Shafi, A. C. Bose, and A. Vinu, "Electrochemical Material Processing via Continuous Charge-Discharge Cycling: Enhanced Performance upon Cycling for Porous LaMnO3 Perovskite Supercapacitor Electrodes," ChemElectroChem, vol. 5, no. 23, pp. 3723–3730, 2018, doi: 10.1002/celc.201801053.
35. P. P. Ma et al., "Effect of A-site substitution by Ca or Sr on the structure and electrochemical performance of LaMnO3 perovskite," Electrochim. Acta, vol. 332, 2020, doi: 10.1016/j.electacta.2019.135489.